

# Effect of Heating Rate on Formability of Ti6Al4V Alloy Micro-gear Under an Electric Field

Yan Xiangzhong<sup>1</sup>, Dan Lei<sup>1</sup>, Yang Yi<sup>1</sup>, Tian Yankang<sup>2</sup>, Huang Kunlan<sup>1</sup>

<sup>1</sup> Sichuan University, Chengdu 610065, China; <sup>2</sup> Centre for Precision Manufacturing and Micro-Manufacturing, University of Strathclyde, Glasgow G1 1XJ, UK

**Abstract:** A novel micro plastic forming technique was introduced to form micro-gears using the high strength, toughness, and hard-to-deform Ti6Al4V alloy materials. The results show that the Ti6Al4V alloy micro-gear can be achieved from a cylindrical Ti6Al4V billet with a set of graphite die under an electric field. The Ti6Al4V material exhibits the best formability when the heating rate is 5 °C/s, while higher heating rate 30 and 40 °C/s can effectively shorten the pre-heating time of materials for deformation. The microstructures of all the formed samples have the Widmanstätten structure, but gear center is in contradiction to tooth top which exhibits a finer microstructure. The  $\beta$  phase content of specimens with the heating rates of 5 and 10 °C/s is slightly higher than that of the original billet, but specimens with heating rates of 20, 30, and 40 °C/s show no  $\beta$  phase from XRD analysis. Moreover, Vickers hardness of all formed samples is higher than that of the original billet under an electric field, and it is independent on the heating rates.

**Key words:** Ti6Al4V alloy; hard-to-deform; electric field; micro-gear; formability

Titanium alloys have been widely used in numerous industrial areas, such as aerospace structures, micro-electromechanical system (MEMS) devices due to their excellent strength, good fracture toughness and corrosion resistance<sup>[1]</sup>. Although showing a high demand, the use of titanium alloy components in these industries is restricted by the poor machining quality since the material is difficult to process<sup>[2]</sup>. Various micro-metal-forming processes have been studied and used to produce different micro titanium alloy components and micro surface structure. For example, Hashigata et al<sup>[3]</sup> produced Au/Ti bi-layered micro-cantilever structure and evaluated its strengthening by micro-bending test. Suman Bhandari et al<sup>[4]</sup> investigated the micro-channel fabrication in titanium alloys by laser ablation and laser-induced plasma micro-machining. Chen et al<sup>[5]</sup> reported that electrochemical machining is an important process to process blisk blades of titanium alloy. The micro-electric discharge machine is used to manufacture complex three-dimensional

features and deep micro-cavities or holes of titanium alloy<sup>[6]</sup>. Nevertheless, all of these methods are used to fabricate the micro titanium alloy components with simple shape or simple surface structure because of the high melting point and low plastic of titanium alloy materials.

Recently, a large number of researchers have studied the effect of electric current on various alloys, and it is found that electric current can effectively improve formability<sup>[7]</sup> and reduce flow stress<sup>[8,9]</sup> for materials with high deformation resistance at relatively lower temperature. Many investigation has also been carried out on microstructural evolution and mechanical properties of alloys affected by electric current, such as microstructural morphology, phase composition, recrystallization, recovery of dislocation, corrosion resistance, and roughness<sup>[10-13]</sup>. However, it has been rarely reported that hard-to-form materials, such as Ti6Al4V titanium alloy, can effectively form micro-parts, let alone complicated parts, based on electric current.

Received date: February 24, 2020

Foundation item: National Natural Science Foundation of China (51705348); Sichuan Science and Technology Program (2019YFG0359); Research Funds for the Central University (2019SCUH0013)

Corresponding author: Huang Kunlan, Ph. D., Associate Professor, School of Mechanical Engineering, Sichuan University, Chengdu 610065, P. R. China, E-mail: huangkunlan@scu.edu.cn

Copyright © 2020, Northwest Institute for Nonferrous Metal Research. Published by Science Press. All rights reserved.

In order to form relatively complicated titanium alloy micro-parts and, at the same time, to simplify the preparing procedure, lower production cost and improve productivity, a new rapid micro-plastic forming technique under an electrical field was proposed by authors to form micro-components of titanium alloy. The process is illustrated in Fig.1. The advantages of this technique over conventional ones include follows: (1) forming mini/micro metal components from hard-to-form metal billet directly; (2) near-net forming; (3) a wide range of metallic plastic material; (4) shorter forming time than other micro forming methods; (5) the process can be easily controlled.

## 1 Experiment

All the specimens had the dimensions of  $\Phi 3.0 \text{ mm} \times 6.65 \text{ mm}$ . The billet was fed into graphite die-set which consisted of an upper punch, a concave die, and a lower punch. Since the die-set plays a critical role in the micro-formability of Ti6Al4V alloy, it was manufactured by precision wire electrical discharge machining. The die-set with the Ti6Al4V billet was subsequently placed into a Gleeble-1500D thermal-mechanical simulation machine from Dynamic System Inc., USA. The billet was expeditiously heated by an electric field with low voltage and high current (3~10 V and 3000~30 000 A) in a vacuum ( $10^{-3} \text{ Pa}$ ) ambient. Then the forming force of 294 N was applied on the upper and lower punches simultaneously and kept constant until the end of the 60 s dwell time. The specific technological parameters for each sample in this study are shown in Table 1.

After air cooling, these formed specimens were mechanically polished to achieve a mirror-like surface and then etched with a solution of 2% hydrofluoric acid, 4% nitric acid and 96% absolute ethyl alcohol for 5 s. The morphologies and microstructural characteristics of formed samples after etching were evaluated by a scanning electron microscope (SEM, JSM-5900LV, JEOL Japan). The X-ray diffraction (XRD, EMPYREAN, Holland) analysis was carried out to investigate the change of phase content, and the hardness was mainly characterized by the Vickers hardness tester.

## 2 Results and Discussion

### 2.1 Apparent morphology of formed samples

Gleeble-1500D thermal-mechanical simulator controls output current according to preset heating speed. The relationship between current and heating rate can be expressed by the following equation:

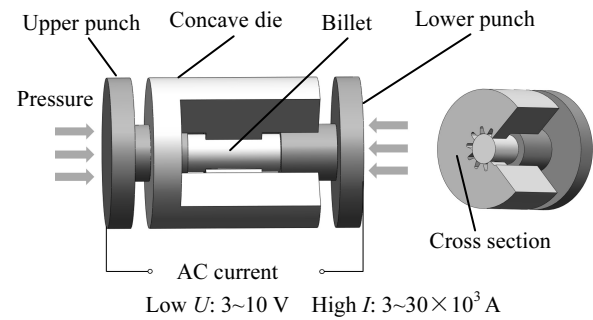


Fig.1 Illustration of the micro plastic forming technique under an electrical field

$$\frac{I}{A} = \sqrt{\frac{\rho C}{\sigma} \cdot \frac{dT}{dt}} \quad (1)$$

where  $I$  is the current passing through the sample,  $A$ ,  $\rho$ ,  $C$ ,  $\sigma$  and  $dT/dt$  are the cross-sectional area, density, specific heat capacity, resistivity coefficient and preset heating rate of sample, respectively. From Eq.(1),  $I^2 \propto dT/dt$  can be easily obtained because  $\rho$ ,  $C$  and  $\sigma$  are material constants related with the materials, and thus, the current magnitude is only related to the heating rate, namely the current increases with the increase of heating rate.

Fig.2a shows the history of stroke and temperature along with time. Under the same forming pressure, it can be seen that the stroke of all the samples starts to take place at about  $660 \text{ }^\circ\text{C}$  even if the heating rates are different. This indicates that severe pure electro-plastic effect caused by high electric current (30, 40  $^\circ\text{C/s}$ ) is more significant in plastic deformation of Ti6Al4V alloy with a relatively shorter time and lower temperature<sup>[14]</sup>. Moreover, the change of stroke for sample 1# during the dwell time slows down, which is different from other samples. This is because the raw material has almost filled the die cavity before the temperature reaches  $1200 \text{ }^\circ\text{C}$ . The lengths of stroke for all samples before and during dwell time are shown in Fig.2b. Note that, as the heating rate increases, more stroke occurs at the forming temperature. The major reason is that, with a relatively shorter period of time before the temperature reaching  $1200 \text{ }^\circ\text{C}$ , Ti6Al4V alloy subjected to electric current is not adequately softened due to dynamic recovery, dynamic recrystallization or phase transformation.

Fig.3 shows the polished micro-gear with a pitch diameter

Table 1 Forming parameters corresponding to the samples formed

| Sample | Heating rate/ $^\circ\text{C} \cdot \text{s}^{-1}$ | Forming temperature/ $^\circ\text{C}$ | Pressure/N | Dwell time at $1200 \text{ }^\circ\text{C/s}$ | Total forming time/s |
|--------|--|---------------------------------------|------------|---|----------------------|
| 1#     | 5  | 1200                                  | 294        | 60  | 300                  |
| 2#     | 10   | 1200                                  | 294        | 60  | 180                  |
| 3#     | 20   | 1200                                  | 294        | 60  | 120                  |
| 4#     | 30   | 1200                                  | 294        | 60  | 100                  |
| 5#     | 40   | 1200                                  | 294        | 60  | 90                   |

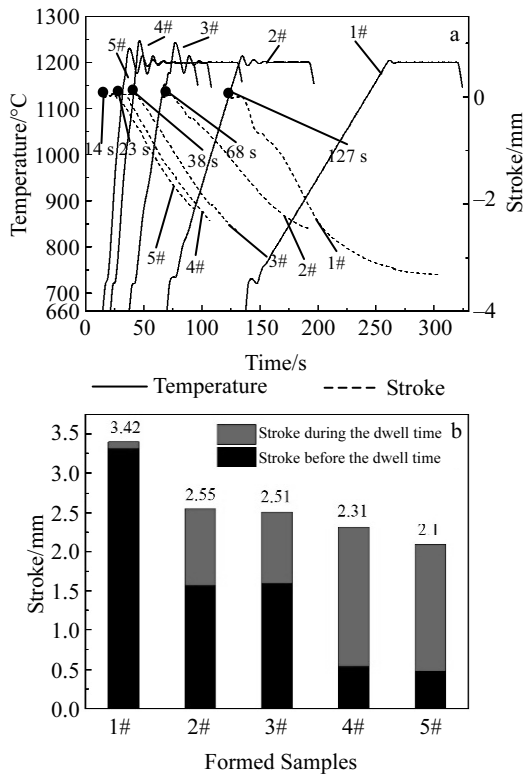


Fig.2 Curves of stroke and temperature vs time (a) and values of stroke (b) of formed samples at different heating rates

of 5 mm formed at the heating rate of 5 °C/s. Fig.4a, 4c~4g exhibit cross-sectional morphologies of the billet and formed samples at different heating rates. Fig.4b, 4h, and 4i are the high resolution images of billet, 4# and 5# samples, respectively. It is noticed that there are holes in the original billet. However, these small cavities can scarcely be found in Fig.4c~4e, which indicates that these cavities can be healed under an electric field. The internal cavities are replaced by newly formed grains, which are achieved by recrystallization and grain growth<sup>[15]</sup>. In contrast to Fig.4c~4e, a couple of holes exist in Fig.4e and 4f. This indicates that grains do not sufficiently grow to fill these cavities in the total forming time of 100 and 90 s.

It is also found that Fig.4c has the clearest and the most

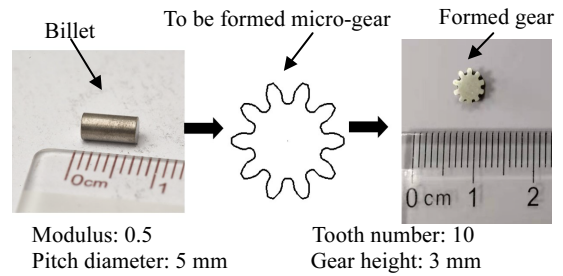


Fig.3 Formed micro-gear under an electric field

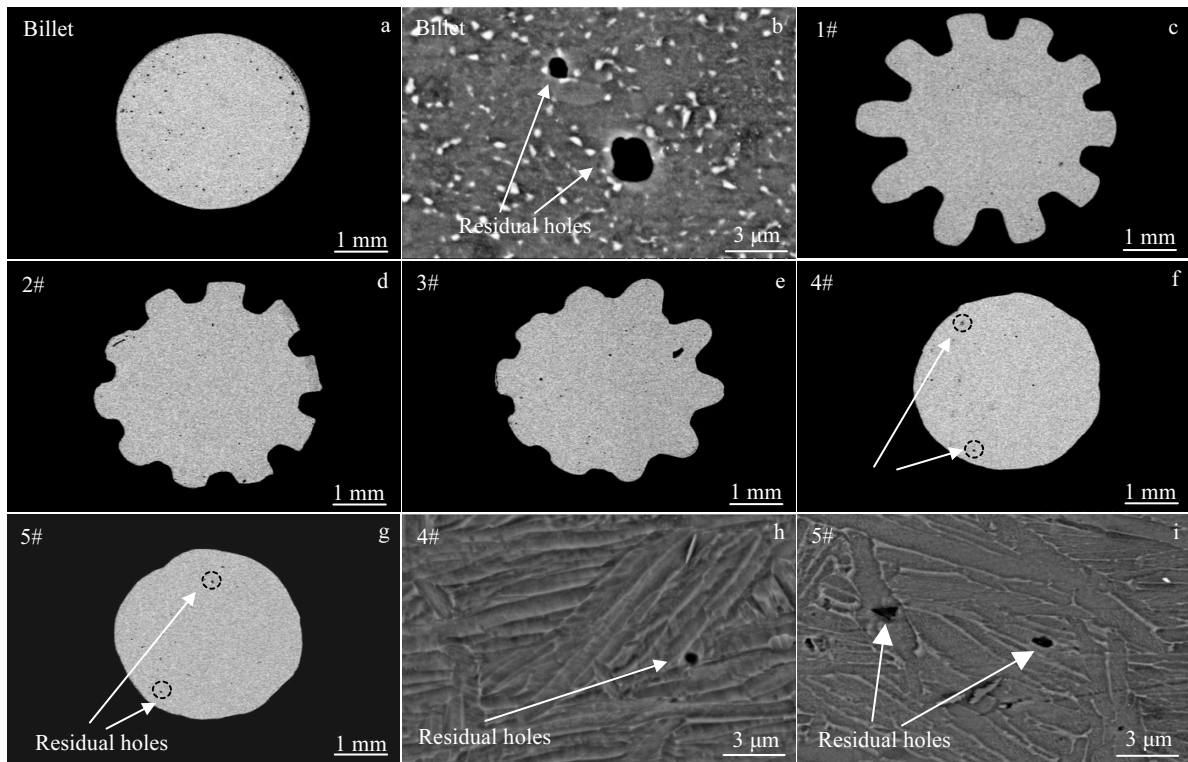


Fig.4 SEM images of cross-section of the billet (a, b) and formed samples (c~i) at different heating rates: (c) 1# at 5 °C/s, (d) 2# at 10 °C/s, (e) 3# at 20 °C/s, (f, h) 4# at 30 °C/s, and (g, i) 5# at 40 °C/s

complete tooth profile compared with Fig.4d~4f and Fig.4g. Fig.4d and 4e show a relatively clear gear profile, whereas Fig.4f, and 4g basically remain the original shape. The morphological characteristics, as mentioned above, can be attributed to the heating rates under an electric field, illustrating that a lower heating rate is conducive to enhance the plastic formability of Ti6Al4V alloy under constant pressure.

## 2.2 Effect of heating rate on phase content

For Ti6Al4V alloy, when temperature increases from a ( $\alpha+\beta$ ) two-phase temperature to a  $\beta$ -phase temperature across  $\beta$ -transus temperature (approximately 995 °C<sup>[16]</sup>), the  $\alpha$ -phase with hexagonal close-packed (hcp) crystal structure in ( $\alpha+\beta$ ) two-phase is completely transformed to a single  $\beta$ -phase (Fig.5) with body-centered cubic (bcc) crystal structure. There are fewer slip systems in hcp unit cell with the three most densely packed lattice planes than in bcc unit cell with the most densely packed {110} lattice planes<sup>[17,18]</sup>. Moreover, the value of self-diffusion coefficient of  $\alpha$  phase is about two order of magnitude lower than that of  $\beta$  phase, so the  $\beta$  phase shows better plasticity than  $\alpha$  phase in the plastic forming conditions<sup>[19]</sup>.

In the present work, the final temperature (1200 °C) of all original billets under an electric field is above the  $\beta$  phase transus temperature. However, with the exception of Fig.4c, other formed samples do not show satisfied shapes, as shown in Fig.4d and 4e, even hold the original shape in Fig.4f and 4g. This is because the forming time is too short to sufficiently complete phase transformation ( $\alpha+\beta\rightarrow\beta$ ). In this study, the total phase transformation time for sample 1# from 895 °C<sup>[20]</sup> to the end of dwell time is about 120 s, which is the longest among all formed samples. The preferable micro-gear profile of this sample benefits from the increment of  $\beta$  phase content. But in contrast, the sample 4# and 5# barely undergo the process of phase transformation in less than 100 s which includes the 60 s dwell time at 1200 °C.

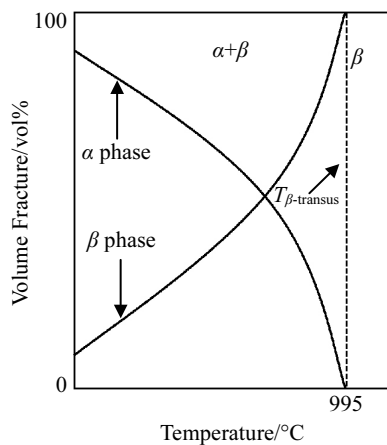


Fig.5 Variation in content of  $\alpha$  and  $\beta$  phase with temperature for Ti6Al4V alloy

Fig.6 shows the XRD patterns for billet material and Ti6Al4V formed samples subjected to different heating rates. Formed samples 1# and 2# exhibit several  $\alpha$  peaks and  $\beta$  peaks, and their  $\beta$  phase content after air cooling is 7.53% and 6.81%, respectively. The calculated XRD peak area of these two samples is a little higher than that of the as-received material, which is 6.72%. However, there are no  $\beta$  peaks for formed samples 3#~5#, in good agreement with the experiment result of Jiang et al<sup>[21]</sup>. This implies that with the aid of high electric current, it is possible to accelerate the  $\beta$  phase transformation to  $\alpha$  phase. A small number of the  $\beta$  phases remaining in the sample may also be hard to detect by XRD.

## 2.3 Microstructure of formed samples

The billet, as shown in Fig.7, has a coarse duplex microstructure comprising primary  $\alpha$  phase (dark area) and  $\beta$  phase (bright area) flake. Back-scattered electron images of tooth top and gear center in formed samples at different heating rates ranging from 5 °C/s to 40 °C/s are shown in Fig.8.

The microstructures of the sample formed by electric field assisted forming above  $\beta$ -transus temperature at 1200 °C are shown in Fig.8. Due to the high temperature and the constant pressure, the grains are elongated and during the air cooling, a mixture of lamellar  $\alpha+\beta$  and  $\alpha$  colonies forms. Although the thickness of the microstructure is different, they all present the

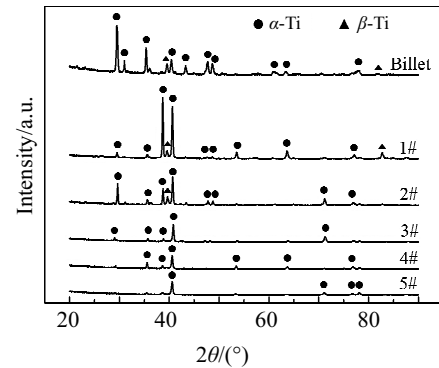


Fig.6 XRD patterns of the formed samples and billet of Ti6Al4V alloy

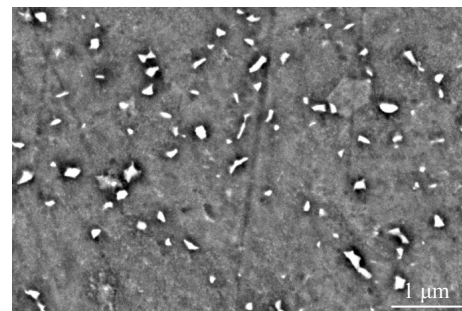


Fig.7 Microstructure of the original billet

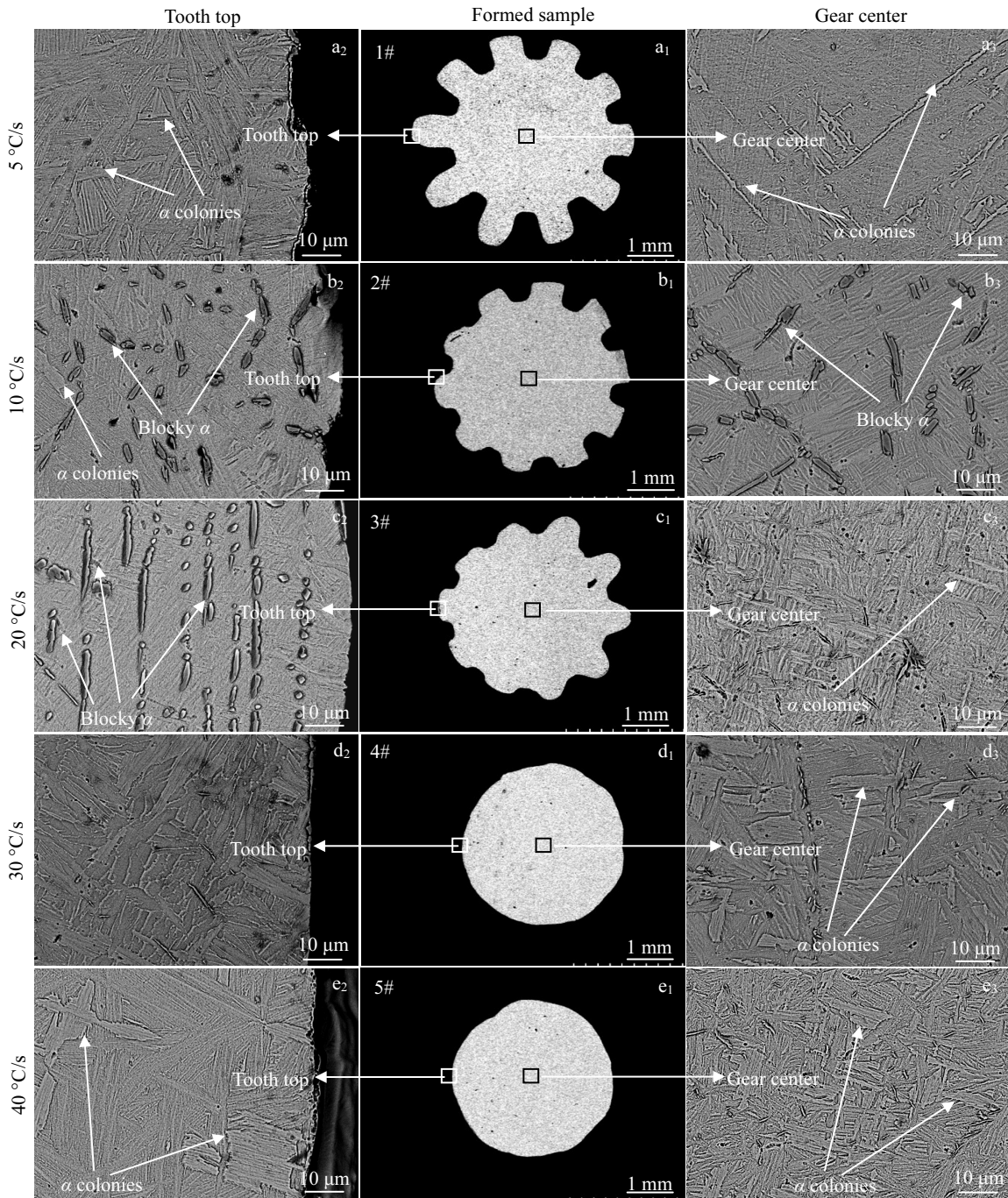


Fig.8 Microstructures of formed samples: (a<sub>1</sub>~a<sub>3</sub>) 1# at 5 °C/s, (b<sub>1</sub>~b<sub>3</sub>) 2# at 10 °C/s, (c<sub>1</sub>~c<sub>3</sub>) 3# at 20 °C/s, (d<sub>1</sub>~d<sub>3</sub>) 4# at 30 °C/s, and (e<sub>1</sub>~e<sub>3</sub>) 5# at 40 °C/s

Widmanstätten structure. A similar microstructure in previous works has been presented by Chicos et al<sup>[22]</sup>.

It can also be found that the microscopic structure of the tooth top is different from that of the gear center. The tooth top of formed samples experiences the most severe deformation during plastic forming under an electric field. This area reveals a finer microstructure while thick lath shape microstructure is found in the gear center where the least

deformation occurs. Furthermore, another possible mechanism contributing to the finer microstructure is the difference of cooling rates between tooth top and gear center zone in air cooling. A higher cooling rate on the surface can also effectively restrict the growth of grains and promote the forming of a finer microstructure.

Meanwhile, blocky  $\alpha$  phase, which exhibits significantly larger and more horned morphologies than primary  $\alpha$ , is found

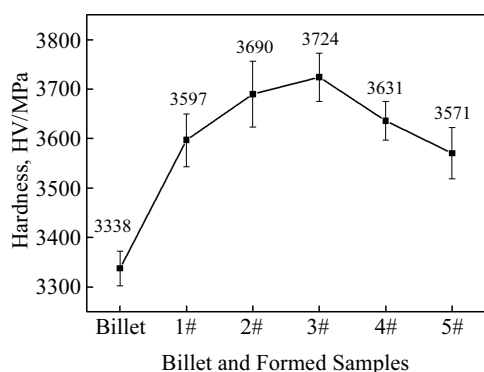


Fig.9 Vickers hardness of the original billet and formed samples

in formed sample 2# and tooth top of 3#, as shown in Fig.8b<sub>2</sub>, 8b<sub>3</sub> and 8c<sub>2</sub>. This is because the Al element, as an  $\alpha$  phase stabilizer, is mainly distributed and accumulated near the grain boundary at the heating rates of 10 and 20 °C/s under constant pressure of 294 N. The  $\alpha$  phase preferentially forms and grows up in the areas rich in  $\alpha$  stabilizing elements, developing to the blocky  $\alpha$  under exterior pressure<sup>[20,23]</sup>.

#### 2.4 Hardness of formed samples

Fig.9 represents the hardness measured at least 8 times for each specimen, in regard to varying heating rates. It shows that the hardness of specimen after air cooling is higher than that of the original billet. Factors influencing the enhancement in hardness have been explored in several studies<sup>[24-27]</sup>. A mixture of high density dislocations, refined grains, deformation twins, density dislocations, and twin boundaries is generated, associated with the process of plastic deformation. Dislocations pile up near the phase boundaries or grain boundaries because of the pinning effect, providing nucleation for new sub-grains and increasing the hardness of the formed samples under an electric field<sup>[24]</sup>. At the same time, the densification of formed samples, as a consequence of the reduction of residual holes under an electric field, is also responsible for the enhanced hardness.

### 3 Conclusions

1) Micro-plastic forming is introduced to fabricate micro-gears using difficult-to-form Ti6Al4V titanium alloy. The micro-gears with the pitch diameter of 5 mm can be produced in the Gleeble-1500D thermal-mechanical simulation machine when the die-set and materials are heated up to a temperature of 1200 °C, with a dwell time of 60 s at a slower heating rate (5 °C/s). Moreover, a higher electric current is beneficial to enhance the formability of Ti6Al4V alloy.

2) The microstructure of the gear tooth is finer than that of the gear center but both shows the Widmanstätten structure. Meanwhile, the heating rate has a major influence on the

forming of blocky  $\alpha$  microstructure.

3) The Vickers hardness of formed samples increases significantly under an electrical field as compared with the original billet.

#### References

- Huang S S, Zhang J H, Ma Y J et al. *Journal of Alloys and Compounds*[J], 2019, 791: 575
- Mohanty S, Kumar V, Das A K et al. *Journal of Manufacturing Processes*[J], 2019, 37: 28
- Hashigata K, Chang T F M, Tang H C et al. *Microelectronic Engineering*[J], 2019, 213: 13
- Bhandari S, Murnal M, Cao J et al. *Procedia Manufacturing*[J], 2019, 34: 418
- Chen X Z, Xu Z Y, Zhu D et al. *Chinese Journal of Aeronautics*[J], 2016, 29(1): 274
- Bellotti M, Qian J, Reynaerts D. *Procedia CIRP*[J], 2018, 68: 610
- Salandro W A, Jones J J, Mcneal T A et al. *J Manuf Sci Eng*[J], 2010, 132(5): 11
- Perkins T A, Kronenberger T J, Roth J T. *J Manuf Sci Eng*[J], 2007, 129(1): 84
- Zhang H, Ren Z C, Liu J et al. *Journal of Alloys and Compounds*[J], 2019, 802: 573
- Bala Srinivasan P, Liang J, Blawert C et al. *Applied Surface Science*[J], 2009, 255(7): 4212
- Kim M J, Lee K, Oh K H et al. *Scripta Materialia*[J], 2014, 75: 58
- Song H, Wang Z J, Gao T J. *Trans Nonferrous Met Soc China*[J], 2007, 17(1): 87
- Zhu Y H, To S, Lee W B et al. *Materials Science and Engineering A*[J], 2009, 501(1-2): 125
- Li D L, Yu E L. *Materials Science and Engineering A*[J], 2009, 505(1-2): 62
- Qiu Y, Xin R S, Luo J B et al. *Materials*[J], 2019, 12(6): 890
- Ding R, Guo Z X. *Materials Science and Engineering A*[J], 2004, 365(1-2): 172
- Quan G Z, Luo G C, Liang J T et al. *Computational Materials Science*[J], 2015, 97: 136
- Lu J Z, Wu L J, Sun G F et al. *Acta Materialia*[J], 2017, 127: 252
- Motyka M, Sieniawski J, Ziaja W. *Materials Science and Engineering A*[J], 2014, 599: 57
- Zeng L R, Chen H L, Li X et al. *Journal of Materials Science & Technology*[J], 2018, 34(5): 782
- Jiang Y B, Tang G Y, Shek C H et al. *Acta Materialia*[J], 2009, 57(16): 4797
- Chicos L A, Zaharia S M, Lancea C et al. *Solar Energy*[J], 2018, 173: 76
- Jiang B Z, Emura S, Tsuchiya K. *Materials Science and Engineering A*[J], 2018, 722: 129
- Ren X D, Zhou W F, Liu F F et al. *Applied Surface Science*[J], 2016, 363: 44
- Mengucci P, Gatto A, Bassoli E et al. *Journal of the Mechanical*

- Behavior of Biomedical Materials[J], 2017, 71: 1  
26 Jiang Y B, Guan L, Tang G Y et al. Materials Science and Engineering A[J], 2011, 528(16-17): 5627  
27 Dong X H, Chen F, Chen S et al. Journal of Materials Processing Technology[J], 2015, 219: 199

## 电场升温速率对 Ti6Al4V 钛合金微齿轮成形性影响

阎相忠<sup>1</sup>, 但磊<sup>1</sup>, 杨屹<sup>1</sup>, 田彦康<sup>2</sup>, 黄坤兰<sup>1</sup>

(1. 四川大学, 四川 成都 610065)

(2. 思克莱德大学 精密制造与微制造中心, 英国 格拉斯哥 G1 1XJ)

**摘要:** 采用电场辅助微塑性模锻成形技术成型了高强度、大硬度、低塑性的 Ti6Al4V 钛合金微齿轮。结果表明, 在电场作用下, 圆柱形 Ti6Al4V 坯料在石墨模具中可以成型微齿轮。Ti6Al4V 材料在加热速率为 5 °C/s 时具有最佳的可成型性, 较高的加热速率 30 和 40 °C/s 可以有效地缩短材料预变形的时间。经电场辅助成型的样品均具有魏氏结构, 但齿顶比齿心的组织更细小。加热速率为 5 和 10 °C/s 的试样  $\beta$  相含量略高于原始坯料, 但加热速率为 20、30 和 40 °C/s 的试样没有显示出  $\beta$  相。此外, 在电场作用下, 所有成形样品的维氏硬度均有所增加。

**关键词:** Ti6Al4V 钛合金; 低塑性; 电场; 微齿轮; 成形性

---

作者简介: 阎相忠, 男, 1992 年生, 博士, 四川大学机械工程学院, 四川 成都 610065, E-mail: lutxiang@126.com